(Preprint) AAS 19-231

NAVIGATION ACCURACY AT JUPITER AND SATURN USING OPTICAL OBSERVATIONS OF PLANETARY SATELLITES

Nicholas Bradley[*], Shyam Bhaskaran[†], Zubin Olikara[‡], Stephen B. Broschart[§]

Autonomous on-board navigation has the potential to enable new types of missions and decrease reliance on NASA's Deep Space Network for navigation purposes. Previous results have shown that navigating with only optical images of asteroids is feasible for inner planet cruise. In this study, we show that images of natural satellites can be used to navigate during approach and tour phases around the gas giants. We investigate the Jupiter and Saturn systems here, and specifically assess the performance of optical-only navigation for the Juno, Europa Clipper, and Cassini trajectories. Early approach phases and tours at Jupiter would require radiometric data to navigate, but the performance of optical-only data rivals the as-flown performance for Cassini at Saturn.

INTRODUCTION

Interplanetary navigation techniques continue to evolve, but change is largely slow and incremental. Missions have long relied on the same staples of navigation techniques: collecting radiometric measurements on the ground (Doppler, range, and Delta Differenced One-Way Ranging [DDOR]), and, in several cases, images taken by the spacecraft. All data is ground-processed to obtain a navigation solution. Almost every interplanetary spacecraft has relied solely on ground-in-the-loop navigation to reach its destination and accomplish its objectives. A few spacecraft have incorporated autonomous on-board navigation, but only briefly and in very restricted mission scenarios.[1]

As mission needs increasingly tax the ground-based antenna network, new missions must compete for the limited resource of ground station time in order to fly successfully. With the advent of new mission concepts, such as CubeSat constellations and Kuiper Belt orbiters, the typical framework of ground-only navigation must be supplemented or entirely replaced with on-board autonomous navigation (AutoNav). In an AutoNav paradigm, a spacecraft collects its own navigation data, computes its own trajectory solutions, and executes maneuvers to keep it on course. Such a concept was demonstrated on the Deep Space 1 mission, which briefly computed its own

[*]Outer Planet Navigation Group, Mission Design and Navigation Section, Jet Propulsion Laboratory, California Institute of Technology. 4800 Oak Grove Drive, Pasadena, California, 91109

[†]Group Supervisor, Outer Planet Navigation Group, Mission Design and Navigation Section, Jet Propulsion Laboratory, California Institute of Technology. 4800 Oak Grove Drive, Pasadena, California, 91109

[‡]Inner Planet Mission Analysis Group, Mission Design and Navigation Section, Jet Propulsion Laboratory, California Institute of Technology. 4800 Oak Grove Drive, Pasadena, California, 91109

[§]Former member, Outer Planet Navigation Group, Mission Design and Navigation Section, Jet Propulsion Laboratory, California Institute of Technology. 4800 Oak Grove Drive, Pasadena, California, 91109. Currently with The Spacing Guild, LLC.

cruise navigation solutions as a proof of concept. Other missions, such as Deep Impact and Stardust, have used AutoNav in terminal guidance to achieve a successful impact with their targets.[1] To date, AutoNav has relied solely on optical images taken by the onboard camera of natural bodies (specifically asteroids and comets) as its data type; this makes the system self-contained and does not require the ground to be in the loop. In principle, a deep space AutoNav system could also incorporate one-way radiometric data, either from the Earth or another spacecraft (spacecraft in the Earth's vicinity could rely on GPS satellites), but this type of one-way radiometric navigation has yet to be demonstrated in practice.

Notwithstanding these flight implementations of AutoNav, there has been little investigation into whether an optical-only AutoNav system could be successful in a wide variety of mission scenarios throughout the solar system. The authors previously examined cruise navigation capabilities throughout the solar system, and found that the inner solar system would be quite amenable to an AutoNav mission, due primarily to the abundance of main-belt asteroids that may be imaged. Similarly, navigation within the asteroid belt is feasible with AutoNav, even with only a modest camera. However, beyond the asteroid belt, the authors found that the lack of visible targets creates a more challenging regime in which to autonomously navigate.[2]

The authors previously examined three different Mars mission scenarios for their AutoNav capabilities: a lander mission (modeled after the InSight mission), a flyby mission (modeled after MarCO), and an orbiter mission (modeled after MRO). The findings support the use of AutoNav for cruise and approach navigation in a flyby and orbiter scenario. The demanding constraints of atmospheric entry mean that only the best available camera class is capable of providing a navigation solution that is sufficient to meet entry interface requirements.[3]

In this paper, we extend the investigation of AutoNav applicability to the gas giants of the outer solar system: Jupiter and Saturn. Even though it has been shown that precise positioning in interplanetary space beyond the asteroid belt is challenging, the natural satellites at Jupiter and Saturn provide ideal imagery candidates for on-board autonomous optical navigation during the approach and tour phases. Using simulated data, we investigate the Juno and Europa Clipper trajectories, and assess the performance against the actual (Juno) and predicted (Europa Clipper) performance of the missions. Similarly, we investigate the Cassini trajectory, from approach through the tour phase, and compare the results to the actual performance. The analysis follows a two-step process, the first being a purely geometric approach by computing the instantaneous positioning accuracy achievable by optical bearing sightings of the satellites, and the second ingesting this data into a full navigation filter. The first step provides an upper bound on the positioning information provided by the data, while the second step mimics the way navigation is typically performed by combining the data into a standard linearized least-squares filter, modeling the complete dynamics of the spacecraft and natural bodies as well as the error sources which affect the data and trajectories. This process estimates, in addition to the spacecraft's position and velocity, other forces which affect the spacecraft's motion. The filter also provides error estimates on the computed orbit, which can be mapped into the future and rotated to various coordinate frames so the performance of the system can be assessed.

MODELING AND ASSUMPTIONS

The results of this paper are intended to be considered in conjunction with previous discussion and results about the AutoNav concept. In particular, the method of determining which targets to observe and the mathematics involved in computing the spacecraft position knowledge are presented

in previous papers.[2,3] In brief, with at least two line-of-sight bearings to natural satellites, the three-dimensional position of the spacecraft can be deterministically computed. If more than two observations are available, all the observations can be combined to obtain a position fix. This result is purely geometric and does not depend on knowing the dynamics of the spacecraft, and is analogous to positioning using GPS satellites. The accuracy of the fix is determined by several factors, including the camera parameters, the ability to determine the exact location of the center of the body (centerfinding), and the accuracy of the target's ephemeris.

For purposes of the analysis presented here, the only target bodies in the database of potential observations are the four Galilean satellites of Jupiter (Io, Europa, Ganymede, and Callisto), and eight of Saturn's largest satellites (Mimas, Enceladus, Tethys, Dione, Rhea, Hyperion, Iapetus, and Phoebe). It was determined with separate analysis that the rest of Jupiter's satellites (for instance, Amalthea) are far too small, and consequently too dim and usually unresolvable, to be of any merit in selecting for an imaging target. Note that at Saturn, Titan is excluded as a target for two reasons: 1) Its thick atmosphere creates potential center-finding inaccuracies, and 2) the Cassini mission performed many close flybys of Titan, and it was desired to remove possible artificially optimistic optical observations during close proximity flybys of Titan.

The cameras used in the analysis here are identical to the cameras used in previous analyses, with the addition of the Cassini Narrow Angle Camera (NAC) for analysis of performance around Saturn. The specifications of these cameras (hypothetical except for NAC, but based on actual cameras) are given in Table 1. In the table, "FOV" is the camera field of view, Θ is the instantaneous field of view (IFOV, or the field of view of a single pixel), M_{max} is the maximum resolvable apparent magnitude, and ψ_{min} is the required keep-out angle between the Sun and an observation target. For all cameras, targets are not included in the analysis if the apparent angular extent between the parent planet's limb and the target is less than 5% of the camera field of view, or if the target is transiting the face of or occulted by the parent body.

Table 1. Spacecraft camera performance parameters

Name	FOV (deg)	Θ (μrad)	M_{max}	ψ_{min} (deg)
Low Res	26.9	128.0	9.5	30
Mid Res	7.0	60.0	10.5	30
Hi Res	0.6	10.0	13.5	30
Cassini NAC	0.35	6.0	14.0	30

The geometric fixes only provide position information; for navigation, it is also critical to know the spacecraft's velocity and the trajectory needs to be propagated into the future for planning maneuvers and guiding the spacecraft to its intended target. To determine the full spacecraft state, a linearized statistical orbit determination filter is applied.[4] The spacecraft trajectory is numerically integrated by modeling all the forces acting on it, the Jacobian matrix of the observation partials are computed around this reference trajectory, and corrections to the parameters estimated in the filter are computed. For analysis, the important result is the covariance matrix describing the uncertainties in the estimated parameters, which typically include the spacecraft position and velocity, plus any maneuvers within the data arc. When reporting a spacecraft state uncertainty, either a current state or a mapped (future) state, that uncertainty depends on the uncertainties of the model parameters used in the navigation filter. In this case, the uncertainties included are observation (data) noise (generally 0.5 pixels 1-σ, unless otherwise noted), and target body ephemeris uncertainty.

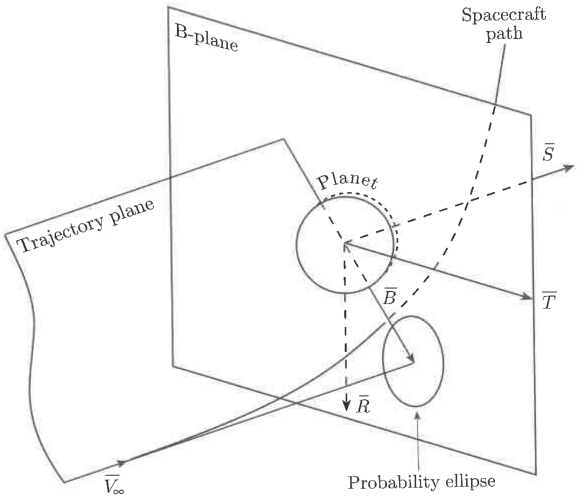

Figure 1. The geometry of the B-Plane.

While the spacecraft state uncertainty is an insightful metric to examine, a possibly more elucidating quantity is the statistical amount of fuel a spacecraft would need to remain on a given trajectory. This is typically done using Monte Carlo techniques; given a schedule of maneuver times, the trajectory uncertainties at the data cutoff prior to each maneuver are sampled and the actual maneuver to achieve the next target location is computed. By performing this statistical analysis for several thousand samples, the statistics of all the maneuvers tells the analyst how much fuel needs to be budgeted to complete a mission. The value needed to fly the reference trajectory to 99% confidence level is typically referred to as the "ΔV99", and is a metric used here to see how well an optical-only system can perform compared to standard ground-based techniques.

Another useful tool to analyze trajectory uncertainty and delivery accuracy is the "B-Plane,"[5] which is a convenient coordinate system in which trajectories and uncertainty ellipsoids can be easily compared. Figure 1 shows the geometry of the B-Plane,[4] which is dependent on the direction of the incoming hyperbolic asymptote. The uncertainty of a spacecraft trajectory in the B-Plane is not truly a physical uncertainty (since the spacecraft does not actually travel to the point at the end of the B vector), but it is useful to compare the ellipse sizes of various cases to show relative uncertainty.

INTERPLANETARY CRUISE TO THE GAS GIANTS

Previous work by the authors presented the feasibility of using optical-based AutoNav in a Solar System-wide context.[3] Asteroids, mostly in the main asteroid belt, were used as imaging targets to determine spacecraft position*. As Figure 2 shows, the number of target asteroids declines rapidly below two (the minimum number required to achieve a valid kinematic position fix) when the spacecraft travels beyond the asteroid belt between Mars' and Jupiter's orbits. Only the Hi Res camera can resolve even a small number of targets in the regime beyond the asteroid belt. The number of visible targets is so small mainly due to the high phase angle of the observation geometry, in addition to the Sun keep-out angle ψ_{min} excluding more and more targets the further from the Sun the spacecraft travels.

*Planets were not included as imaging targets due to likely center-finding difficulties.

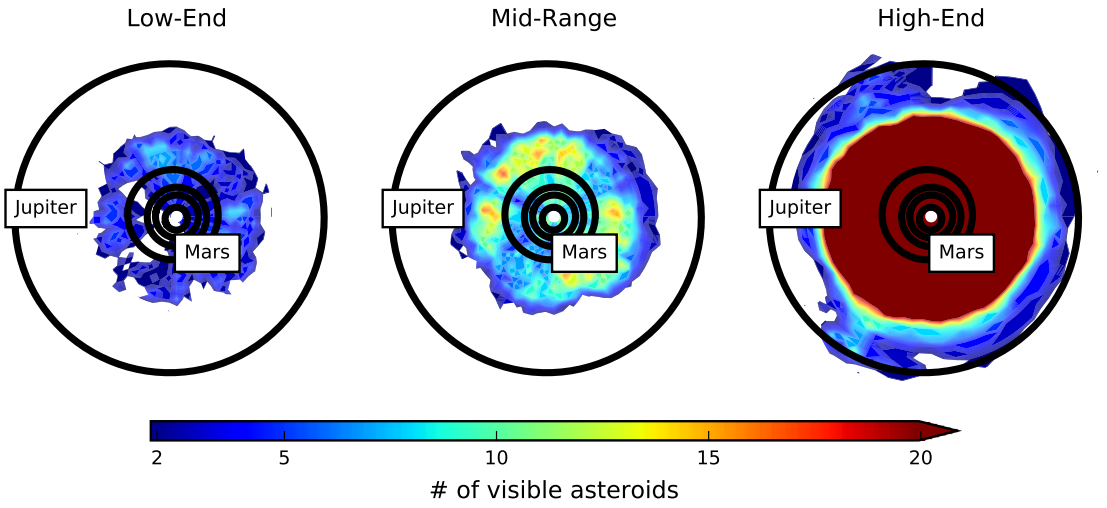

Figure 2. Number of visible asteroid targets by camera type for spacecraft locations in the ecliptic plane, out to the orbit of Jupiter ($N \geq 2$). Beyond Jupiter's orbit, $N < 2$ for all locations.

Because of the dearth of visible navigation targets beyond the main asteroid belt, using solely optical measurements during cruise to the gas giants is difficult within current modest camera capabilities, unless the targets include planets. However, it may not be necessary to perform navigation during the deep space cruise of spacecraft bound for the outer planets. Trajectory correction maneuvers (TCMs) are typically performed in the inner solar system, during the few months following launch. The data cutoffs for these maneuvers usually occur when the spacecraft has a wealth of optical targets to observe, resulting in high-quality navigation solutions. Once the TCMs are executed, there is generally very little need to correct the course of the spacecraft before approach at the target body. If using AutoNav, a spacecraft could use asteroid targets when performing inner solar system TCMs, and use natural satellites on approach to target bodies, as the analysis below shows.

Some flight projects (e.g. New Horizons and Rosetta) have used varying levels of spacecraft hibernation before arrival at their target, some relying on simple "dead reckoning" navigation to determine the state of the spacecraft in the months or years during hibernation.[6,7] For a spacecraft relying on AutoNav to reach the outer planets, hibernation is a possibility during deep space cruise until the natural satellites of the target body are resolvable in the camera. Another possibility for navigating in deep space during this cruise period is to rely on classical radiometric navigation techniques, as most missions have (including Juno and Cassini). The number of radiometric data tracks could potentially be significantly reduced (e.g. one or fewer tracks per week) to provide some coarse level of navigation before the AutoNav could take over during the approach phase.

In summary, using AutoNav with near-Earth or main belt asteroids is difficult or impossible during cruise beyond the asteroid belt, but this fact is not a barrier to using an optical-based AutoNav on an outer planet mission. Deep space hibernation or sparse radiometrics can sustain a spacecraft's navigational needs until the approach phase is reached.

JUPITER APPROACH

In the following sections, the detailed analysis of an optical-based AutoNav system for Jupiter approach and satellite tours are presented using the Juno and Europa Clipper missions as a reference.

Juno Approach

The Juno spacecraft performed its insertion burn into orbit around Jupiter (Jupiter Orbit Insertion, or JOI) on July 5, 2016 (UTC). In the months prior to orbit insertion, accurate navigation solutions were required in order to design the orbit insertion maneuver and predict the subsequent Jupiter-centered orbit.

To revisit the JOI scenario with AutoNav capability, it is necessary to generate an imaging schedule for the months prior to approach and arrival at Jupiter. A sample observation schedule for the three cameras is given in Table 2. In this selected image cadence, an image opportunity occurs once every ten days during the first month, once every five days during early approach (until one month prior to insertion), and once every day until two days prior to insertion. Thereafter, image opportunities are allowed every four hours. At an image opportunity, it is not guaranteed that any targets will be visible, due to the camera limitations and spacecraft geometry relative to the targets, Jupiter, and the Sun.

Table 2. Example schedule for the three cameras during Juno's approach to Jupiter. I=Io, E=Europa, G=Ganymede, C=Callisto.

Image time (2016, ET)	Low Res				Mid Res				Hi Res			
	I	E	G	C	I	E	G	C	I	E	G	C
13-APR 21:00								✓		✓	✓	✓
23-APR 21:00									✓	✓	✓	✓
03-MAY 21:00									✓	✓	✓	✓
13-MAY 21:00								✓		✓	✓	✓
18-MAY 21:00									✓	✓	✓	✓
23-MAY 21:00							✓	✓	✓	✓	✓	✓
28-MAY 21:00										✓	✓	✓
02-JUN 21:00							✓	✓	✓	✓	✓	✓
07-JUN 21:00							✓	✓	✓	✓	✓	✓
08-JUN 21:00								✓	✓	✓	✓	✓
09-JUN 21:00							✓	✓	✓	✓	✓	✓
⋮	⋮	⋮	⋮	⋮	⋮	⋮	⋮	⋮	⋮	⋮	⋮	⋮
04-JUL 01:00	✓		✓	✓	✓	✓	✓	✓	✓	✓	✓	✓
04-JUL 05:00			✓	✓	✓	✓	✓	✓	✓	✓	✓	✓
04-JUL 09:00	✓	✓	✓	✓	✓	✓	✓	✓	✓	✓	✓	✓
04-JUL 13:00	✓	✓	✓	✓	✓	✓	✓	✓	✓	✓	✓	✓
04-JUL 17:00	✓	✓	✓	✓	✓	✓	✓	✓	✓	✓	✓	✓
04-JUL 21:00	✓	✓	✓	✓	✓	✓	✓	✓	✓	✓	✓	✓
⋮	⋮	⋮	⋮	⋮	⋮	⋮	⋮	⋮	⋮	⋮	⋮	⋮

Using only these scheduled images of the Galilean satellites, optical observables were simulated and were processed in a navigation filter to determine the current and mapped (future) state un-

certainties of the spacecraft, using the three different cameras. Depending on the resolution and sensitivity of the camera, the Galilean satellites become valid observation targets at different times in the approach to Jupiter. For instance, the Low Res camera cannot resolve any of the four satellites until June 17, 2016, a mere 2.5 weeks before the orbit insertion maneuver. By contrast, the High Res camera can resolve targets immediately when the simulation begins on April 13, 2016.

Figure 3 shows the current state uncertainty of the Juno spacecraft along its approach trajectory using each of the three cameras and the observation schedule in Table 2. Additionally, the actual performance of the ground-based radiometric-only solution from the as-flown trajectory is shown for comparison. While it is clear that the radio-only solution generally outperforms all of the optical-only solutions, the solutions become quite similar in the last week prior to orbit insertion (July 5, 2016), and the Hi Res camera even outperforms the position uncertainty of the radio-only solution in the few days before orbit insertion.

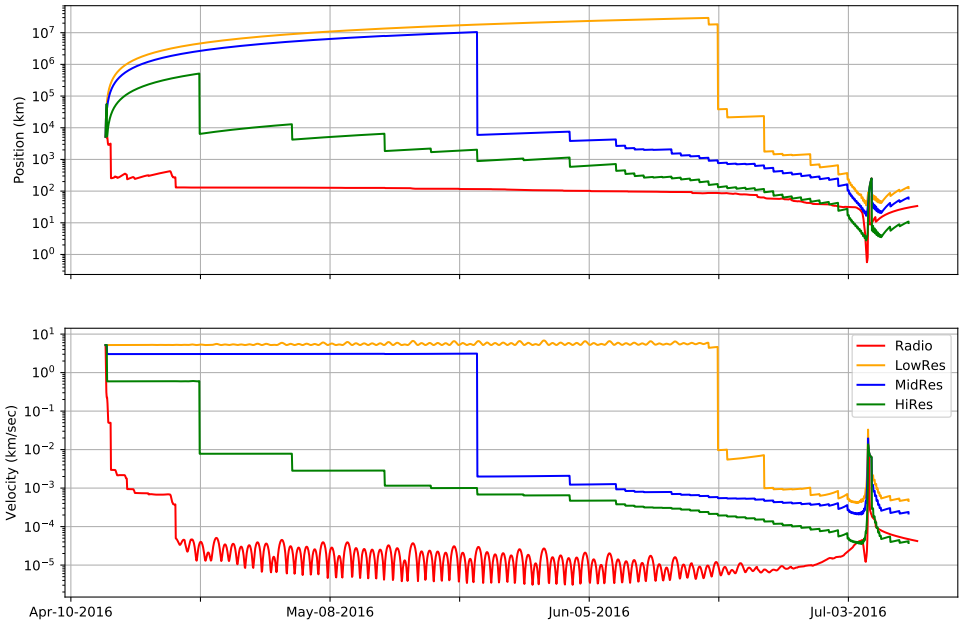

Figure 3. Current state uncertainty for the Juno approach trajectory.

To obtain the ΔV99 value, we analyzed four maneuvers, three statistical (TCM-12 [pre-JOI], TCM-13 [pre-JOI], and JOI-CLN [a cleanup maneuver after orbit insertion]) and one deterministic (JOI). These maneuvers are given in Table 3, showing the radio-only ΔV99 results along with the results using each of the three AutoNav cameras.

Table 3. ΔV99 analysis for Juno maneuvers.

Name	Time (2016, ET)	Nom. Mag. (m/s)	Maneuver ΔV99 (m/s)			
			Radio-only	Low Res*	Mid Res	Hi Res
TCM-12	31-MAY 18:00:00	0	1.607	—	4.611	1.619
TCM-13	20-JUN 18:00:00	0	10.671	—	58.053	13.490
JOI**	5-JUL 02:31:08	542.1086	—	—	—	—
JOI-CLN	13-JUL 18:00:00	0	23.766	—	132.521	36.613
		Total***	30.806	—	190.360	47.189

* Because the Low Res camera cannot resolve any targets prior to TCM-12, its ΔV99 values are nonsensically high.

** JOI is designed only once and fixed due to the highly nonlinear nature of the first Jupiter periapsis, where JOI is performed.

*** Note that the total statistical ΔV99 is not equal to the sum of the individual ΔV99s.

Table 3 shows that using the Hi Res camera provides comparable results to the radio-only solution, requiring only an extra 16.4 m/s of extra ΔV capability to meet the 99th percentile statistical expectation for accurate insertion into orbit around Jupiter. The Mid Res camera requires nearly 160 m/s of extra capability, so relying on images from the Mid Res camera alone would likely not be feasible for Jupiter orbit insertion. The results could be improved, possibly significantly, if a small amount of radiometric data were included at opportune times, such as just prior to the maneuver data cutoffs. The Low Res camera is not feasible to use for Jupiter orbit insertion because of its inability to resolve the Galilean satellites until just 2.5 weeks prior to orbit insertion.

The 3-σ B-Plane ellipses for the TCM-13 data cutoff (the final statistical maneuver prior to JOI) are shown in Figure 4. Subplot (a) shows all the ellipses, including the radio-only ellipses, compared to the Jupiter impact radius. Subplot (b) zooms to show just the ellipses without the impact radius. Subplot (c) zooms to show only the radio-only solution compared to the Hi Res camera solution. To the right of each subplot is a "Linearized Time Of Flight" plot, which shows a timing uncertainty quantity related to the periapsis timing uncertainty.

From a B-Plane perspective, both the Mid Res and Hi Res cameras are more than sufficient to perform a safe orbit insertion at Jupiter without the risk of impacting the planet. Due to the large ΔV99 for the Mid Res camera, however, an AutoNav system would likely need to carry a camera with similar performance to the Hi Res camera to feasibly achieve orbit around Jupiter both safely and efficiently. The downtrack uncertainty, represented by the linearized time of flight, is larger for the optical-only solutions than for the radio-only solution. An inherent limitation of optical-only results is that they allow for good observability in the plane-of-sky, but not in the spacecraft-to-target direction. Radiometric data allows for observability in the Earth-to-spacecraft line-of-sight, which is generally decoupled from spacecraft-to-target geometry. Because of this decoupling, radiometric data is often able to resolve spacecraft states quite well in all directions when the spacecraft is orbiting a target body, but optical-only data solutions tend to have more uncertainty in the downtrack direction because of the geometric coupling.

Europa Clipper Approach

The Europa Clipper approach results are similar to the Juno approach results, so most of the background information is excluded in this subsection. The Europa Clipper approach trajectory

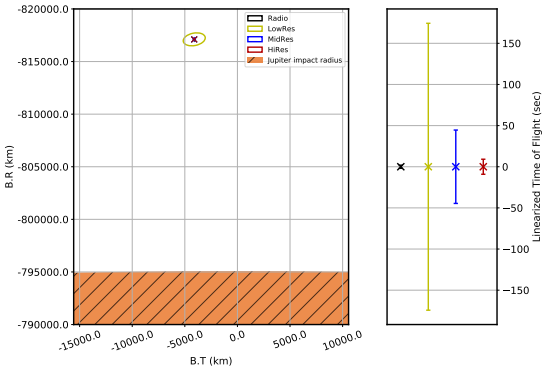

(a) Ellipses compared to the Jupiter impact radius.

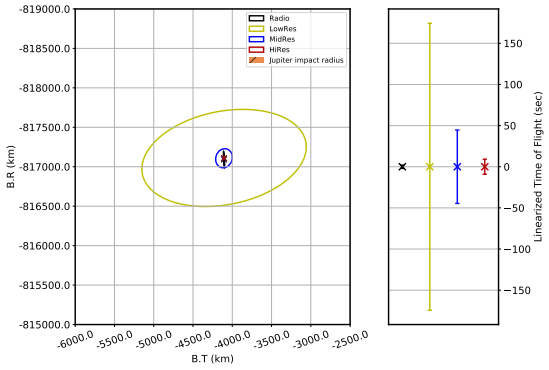

(b) Zoom from (a) showing just the ellipses.

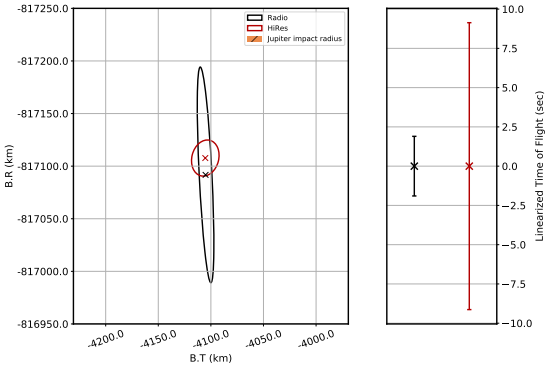

(c) Zoom from (b) showing radio-only compared to Hi Res.

Figure 4. B-Plane ellipses (3-σ) for radio-only and the three camera solutions for TCM-13 (final maneuver prior to JOI). Subfigures zoom in from (a) to (c).

analyzed here is for a 2022 launch date*, and includes three statistical approach maneuvers (G0-APR1, G0-APR2, G0-APR3), all targeting an initial hyperbolic flyby of Ganymede just prior to JOI. As with Juno, only images of the four Galilean satellites are used in the optical-only solutions. Observables are only generated if the relative geometry of the spacecraft and moons satisfy certain constraints (outside the solar keep-out angle, and more than 5% of the camera's FOV off the limb of Jupiter). Data cadence is similar to the Juno approach simulation: image opportunities are provided every 10 days starting on 8-MAY-2024 until 2-NOV-2024, every 5 days until 21-NOV-2024, every day until 21-DEC-2024, and every four hours thereafter until the first flyby on 24-DEC-2024.

Figure 5 shows the current state uncertainty of the approach trajectory using each of the three cameras. It is again apparent here how the Low Res camera does not resolve any targets until very soon before orbit insertion, but that the Hi Res camera is able to resolve targets at the beginning of the simulation. The Hi Res camera produces a current state knowledge of single-digit kilometers in the days before orbit insertion.

Figure 6 shows the B-Plane performance for the Europa Clipper approach trajectory at the first Ganymede flyby (G0). Subplot (a) shows a comparison of the performance of the three cameras for the final approach maneuver, and subplot (b) shows the reduction in B-Plane delivery uncertainty

*The launch for Europa Clipper is currently planned for 2023.

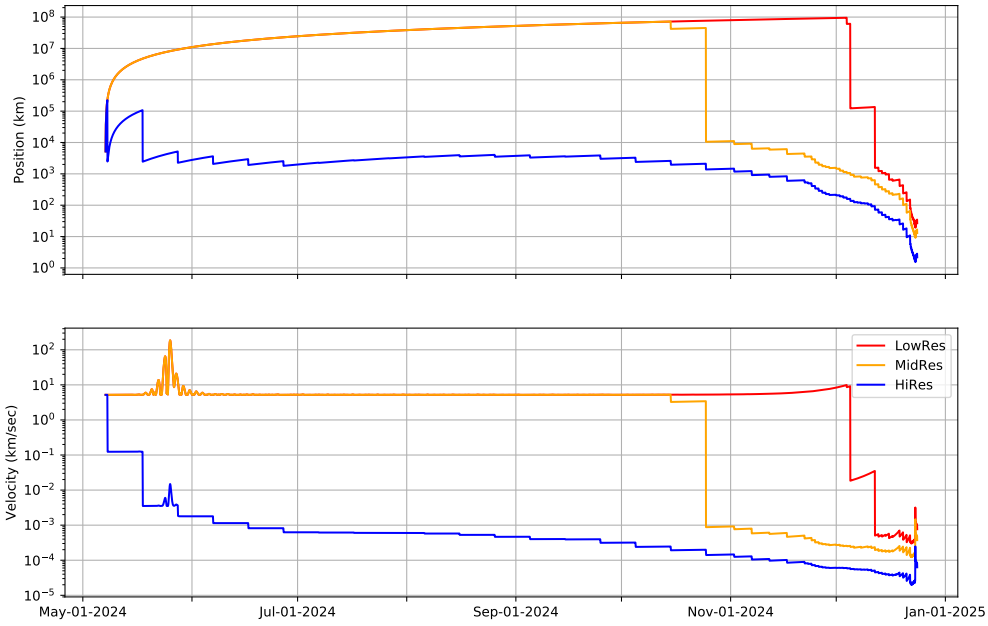

Figure 5. Current state uncertainty for the Europa Clipper approach trajectory.

for the Hi Res camera through the three maneuvers (G0-APR1 through G0-APR3). The G0 flyby occurs on 24-DEC-2024 in this reference trajectory, and the final approach maneuver data cutoff is on 17-DEC-2024.

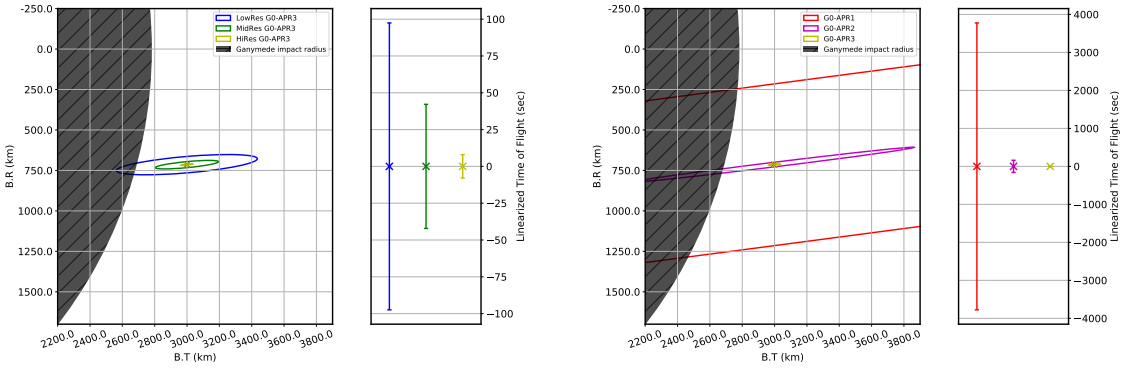

(a) Comparison of camera performance at the final maneuver (G0-APR3) data cutoff.

(b) Reduction of ellipse uncertainty for the Hi Res camera through the three approach maneuvers.

Figure 6. B-Plane ellipses (3-σ) for the first Ganymede flyby (G0), prior to JOI.

The performance of the three cameras (subplot (a)) is quite good for this initial flyby of Ganymede. While the Low Res camera's 3-σ ellipse overlaps the Ganymede impact radius slightly, the Mid Res and Hi Res cameras leave a good amount of statistical margin against impact during the flyby. The

linearized time of flight uncertainty is as low as approximately 10 seconds 3-σ with the Hi Res camera. All cameras benefit from late-breaking navigation updates allowed by the AutoNav framework, at a time when even the Low Res camera has performed sufficient observations to reduce the current state uncertainty to hundreds of kilometers. With the G0 flyby as a comparison metric, all three cameras are capable of navigating from the final approach maneuver cutoff through the first Ganymede flyby.

Subplot (b) shows that for the Hi Res camera, the uncertainty collapses considerably from the G0-APR1 data cutoff (25-JUN-2024) through the G0-APR2 cutoff (22-NOV-2024), and finally to the G0-APR3 cutoff (17-DEC-2024). The consistency of the blue line in Figure 5 shows that this reduction in B-Plane uncertainty is not due to being able to resolve more target bodies, but is related to the propagation of uncertainty through the "time-to-go" between the maneuver data cutoff and the G0 flyby. The 3-σ ellipses of the G0-APR1 and G0-APR2 data cutoffs have a large amount of overlap with the Ganymede impact radius, and the solution would likely improve with the addition of a small amount of radiometric data just before the maneuver data cutoffs.

In all, the Europa Clipper approach trajectory could largely rely on an AutoNav system to perform the first flyby and proceed toward JOI. All three cameras are promising candidates for implementing such a system, but early approach maneuvers could benefit from a small amount of traditional radiometric data. Once the Galilean satellites can be resolved by the cameras, however, the current state knowledge and mapped B-Plane uncertainties are reasonably good.

TOURS

Tours within the Gas Giant planetary systems represent an interesting case study for the use of optical-based AutoNav system. The tours are typically quite long (over 14 years for Cassini when including all the mission extensions), and involve fairly intensive operations due to encounters of the satellites occurring on scales of weeks. Thus, the state-of-the-art requires a large team to perform navigation solutions because deviating from the reference tour due to navigation issues (such as missing the targeted location for a satellite flyby) is expensive in terms of fuel. To perform first-time tour missions, such as Galileo at Jupiter and Cassini at Saturn, ground-based optical measurements are crucial because the ephemerides of the satellites are not known accurately enough to use solely radiometric data, and the optical data enables improvements in those ephemerides (for subsequent tours, such as with Europa Clipper, the need for optical data is still being evaluated). The question addressed here is whether a purely optical AutoNav can support the stringent navigation requirements presented by the tour; if it can, then the burden on ground navigation teams could be reduced, and missions could potentially be flown at a faster cadence of flybys enabled by rapid onboard turnaround for navigation solutions. As shown in the analysis that follows, Jupiter and Saturn are quite different in terms of whether or or not optical AutoNav can perform satisfactorily in their respective planetary systems. In the subsequent sections, we first present a generic geometric analysis of the positioning accuracy in the Jovian and Saturnian systems, followed by a more detailed analysis using the Europa Clipper reference trajectory and the as-flown Cassini trajectory as representative samples.

Kinematic position-only solution at Jupiter

In general, the Jupiter system does not lend itself well to instantaneous kinematic solutions for spacecraft position. The fact that there are only four reasonably visible moons and the need for relative angular separation of imaging targets means that the geometry is sometimes not favorable

to perform kinematic position solutions. However, inside the orbit of Ganymede, the relative separation of the moons and the proximity to the imaging targets can temporarily result in favorable regions for low uncertainty in instantaneous position solutions.

Figure 7 shows the uncorrelated 1-σ uncertainty of locations in the Jupiter system at a representative epoch using the Hi Res camera. The colored contour lines depict different 1-σ instantaneous position uncertainty values. For example, inside the orbit of Ganymede, the kinematic uncertainty is usually approximately 10 km 1-σ. Outside the orbit of Ganymede, the instantaneous uncertainty is sometimes better than 100 km, but there are many "patches" where uncertainty exceeds hundreds or even thousands of kilometers. The empty patch to the left of Callisto is a region in which less than two moons are visible at this particular epoch, and a kinematic solution cannot be obtained. In this case, the Sun is to the right of the figure, and if the spacecraft is to the left of Jupiter, the moons can be lost in the keep-out zone around the Sun (30 degrees, in this case).

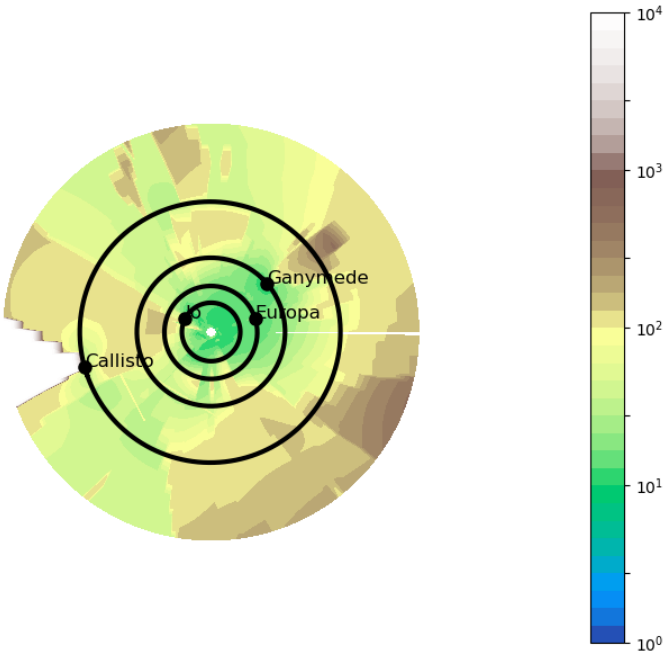

Figure 7. Kinematic 1-σ position accuracy (in km) around Jupiter on 08-AUG-2016 for the Hi Res camera.

Europa Clipper

An analysis of the kinematic position uncertainties was also performed along the entire span of the Europa Clipper tour around Jupiter. This tour starts in December 2024 and extends to September 2028, and includes multiple flybys of Europa and Ganymede.[8] For this analysis, we used the heuristic selection criteria on the four Galilean satellites, sampled every 4 hours, to find the best set to use at each time. We excluded targets within a 30 deg cone angle of the Sun, or whose size filled over 80% of the camera FOV, or would be imaged less than 25% of the camera FOV off the limb of Jupiter. In the resultant set, the kinematic position uncertainty was computed as long as at least two targets remained. The result is shown in Figure 8, showing the uncertainty for all three sample cameras. From January 2025 through May 2026, the spacecraft orbit takes it well outside the realm of the Galileans. During this time, the geometry is poor due to the large distances to the satellites, and

the position uncertainties range from the several thousand kilometers for the Hi Res camera to over 100,000 km for the Low Res. There are also large gaps where one or more of the selection criteria are violated and there are gaps where no kinematic positioning is possible. After this point, the tour places the spacecraft orbit largely in the inner realm of the Jovian system, with the apoapses just outside the orbit of Callisto and the periapses near Europa's orbit radius. The overall uncertainties are much better, with the Hi Res camera levels staying in the 10-100 km range, and the MidRes not much worse with maximum errors of around 1000 km. The LowRes drops as low as 50 km, but the worst case is still over 100,000 km, so the Low Res camera is not a viable option for this particular application. With this background, we now analyze the full filter results and compare them against the baseline reference mission using radiometric data.

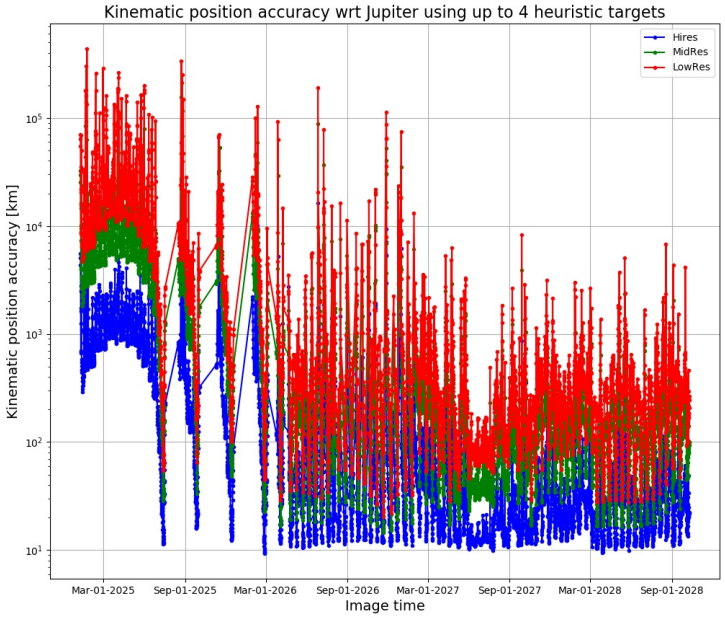

Figure 8. Kinematic 1-σ position accuracy (in km) for the span of the Europa Clipper Tour.

We analyzed the Europa Clipper tour using the full navigation filter setup for trajectory uncertainties as well as the ΔV statistics. Because the Europa Clipper tour is quite long and encompasses 60 flybys of the Galilean satellites, we chose to avoid detailed analysis of each individual flyby for navigation performance and instead focus on the overall result. We accomplish this as shown in Figure 9, which shows a comparison of relevant B-Plane parameter uncertainties between the optical-only cases and the baseline radio-only case at the data cutoff for the final approach maneuver before each flyby. The figure shows the ratio of the B-Plane uncertainty ellipse semimajor axis (SMAA), semiminor axis (SMIA) and time of close approach (TCA).

In all cases, the optical-only performance is worse than the radio-only performance. Using the Low Res camera results in an increase in delivery uncertainty of a factor of 100 times or greater. Even the Hi Res camera, taking images every 4 hours, averages around a factor of 10 times increase in the delivery uncertainty.

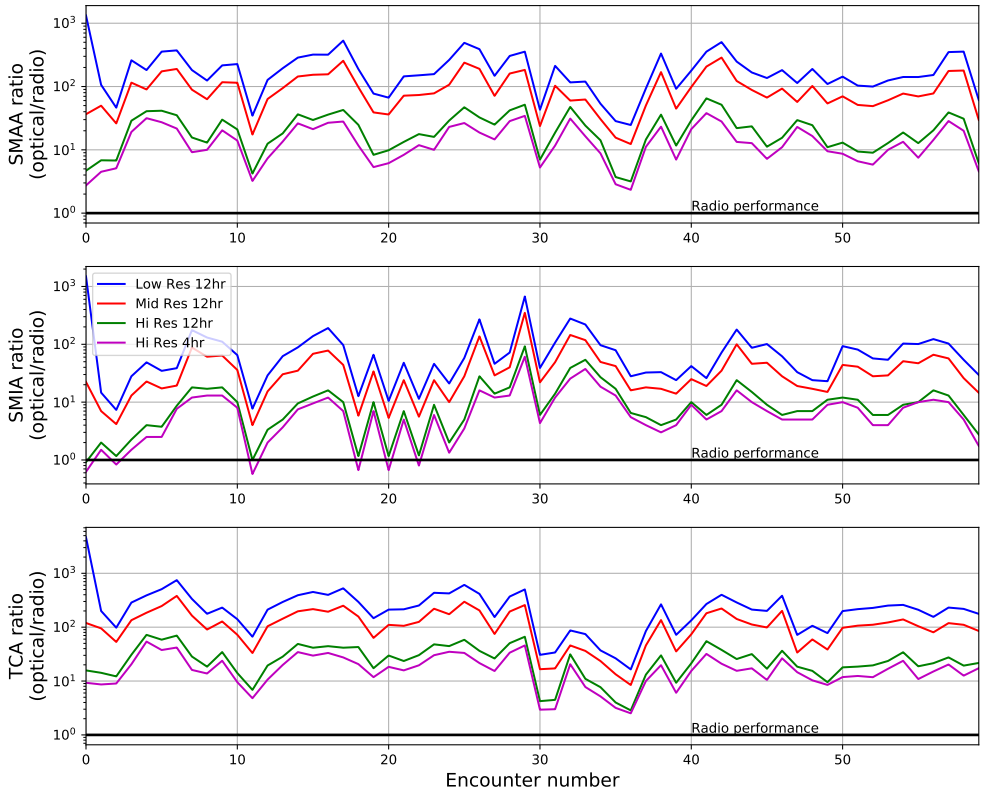

Figure 9. Europa Clipper B-Plane uncertainty comparison for all 60 flybys in the tour. The top figure shows the uncertainty ellipse semimajor axis (SMAA) radio, the middle figure shows the semiminor axis (SMIA) ratio, and the bottom figure shows the time of close approach (TCA) uncertainty ratio.

Table 4. ΔV99 values for the Europa Clipper tour phase, for different cameras compared with the baseline radio-only solution. The deterministic ΔV is 352.39 m/s.

Case	Image frequency	ΔV99 (m/s)
Radio-only	—	448.03
Low Res	12 hr.	35645.56
Mid Res	12 hr.	32162.84
Hi Res	12 hr.	919.58
Hi Res	4 hr.	734.21

Table 4 shows the statistical ΔV99 for the entire tour (based on a representative reference trajectory), comparing the baseline radio-only solution with the results using simulated image observables from the three cameras. The radio-only case was obtained by running the covariance analysis software, provided by the mission's Navigation Team (for details, see Tarzi et al[9]). The Low Res and Mid Res cameras are demonstrably infeasible for the Europa Clipper tour, given their enormous sta-

tistical ΔV99 values greater than 30 km/s. The Hi Res camera offers more acceptable performance, but produces a ΔV99 value over twice the radio-only value if an image cadence of one per 12 hours is assumed. If the image cadence is improved to once every four hours, the ΔV99 improves, but is still significantly higher than the radio-only value. The poor performance of the cameras compared to the radio solution is likely due to the sheer number of maneuvers planned during the tour phase for the Europa Clipper mission. There are 60 planned flybys of the Galilean satellites, each of which requires targeting, approach, and cleanup maneuvers. When using a camera for navigation, even a modest per-maneuver increase in ΔV99 results in a large overall increase in the statistical maneuver uncertainty.

The large increase in statistical ΔV99 combined with the relatively poor delivery in the B-Plane of each flyby shows that the Europa Clipper trajectory is not amenable to using only optical AutoNav to navigate. The number of flybys and associated maneuvers, combined with the very low-altitude flybys, necessitate a more accurate navigation approach. Incorporating some amount of radiometrics or improving camera technology are two possible avenues for improvement, but the scarcity of visible moons to observe at Jupiter means that an optical-based AutoNav system cannot perform at the same level as a radio-navigated mission, at least for this particular mission. It is quite possible, however, that a different scenario might be amenable to AutoNav with reasonable performance.

Kinematic position-only solution at Saturn

The Saturnian system is more suitable than the Jovian system for using AutoNav. Figure 10 shows the uncorrelated 1-σ position uncertainty for locations in the Saturn system at a certain representative epoch using the Hi Res camera. The colored regions depict different 1-σ instantaneous position uncertainty values. Saturn has enough sufficiently-visible targets that the position uncertainty around the planet is lower (better) and more uniform than at Jupiter. Inside the orbit of Titan, the 1-σ uncertainty can be at or below 10 km. Outside Titan's orbit, the 1-σ uncertainty can climb to hundreds of kilometers, but does not exceed 1000 km, even well outside the orbit of Iapetus. Overall, the Saturnian system is a more promising candidate than Jupiter for optical-based AutoNav.

Cassini

The Cassini tour at Saturn is analyzed next. For this analysis, we make one adjustment in that the optical analysis is performed with the camera that was flown on the spacecraft (Narrow Angle Camera, or NAC), rather than using the generic Low, Mid, or Hi Res cameras. The NAC has nearly twice the resolution (and narrower overall FOV) than the generic Hi Res camera (see Table 1). As with the Europa Clipper analysis, the bounding case for current position uncertainty is to use an uncorrelated kinematic position fix. Figure 11 shows the kinematic position uncertainty for the full 13-year mission at Saturn, evaluated every four hours along the as-flown trajectory.

Before Saturn Orbit Insertion (SOI), the natural satellites of Saturn are quite distant, and small uncertainties in the camera optics translate to large position uncertainties. Additionally, only the satellites with the largest elongation from Saturn's limb can be imaged, due to the constraint that targets must be greater than 5% of the camera field of view from a planet's limb. As Cassini approaches Saturn and nears SOI, the spacecraft position uncertainty drops dramatically, as more moons are visible and the pixel error of the image translates into a smaller translational uncertainty. At the time of orbit insertion, a kinematic position calculation can achieve a 1-σ accuracy of less than 10 km.

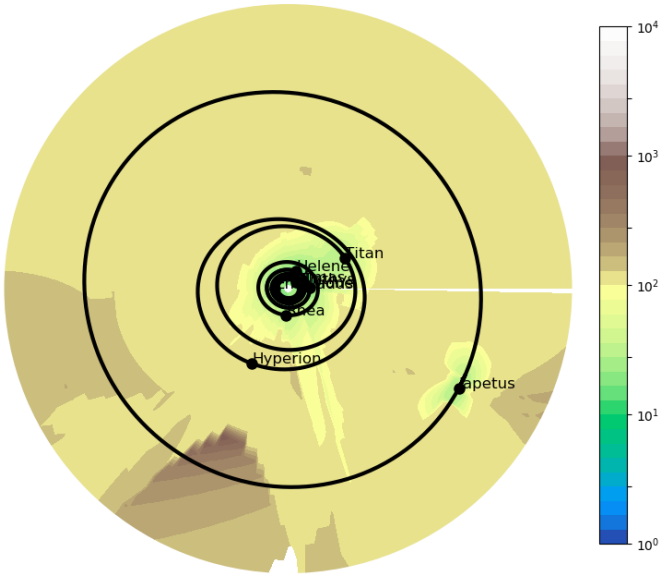

Figure 10. Kinematic 1-σ position accuracy (in km) around Saturn on 30-JUL-2016 for the Hi Res camera.

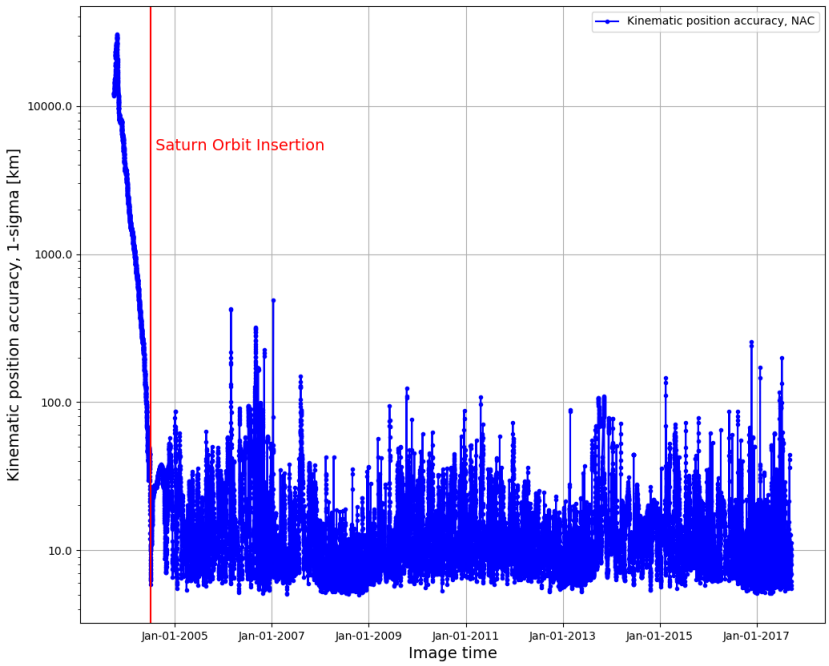

Figure 11. Kinematic position accuracy for the entire Cassini mission at Saturn, using up to six image targets per data point, for the Cassini Narrow Angle Camera (NAC).

As the tour progresses, the accuracy of the kinematic solution ranges from single kilometers to several tens of kilometers. There are several instances when the uncertainty exceeds 100 km, but these are by far the exception rather than the norm. Contrast this result to the Europa Clipper analysis in Figure 8, where even for the Hi Res camera, the uncertainty is frequently in the hundreds of kilometers, and never drops appreciably below 10 km.

We also performed the complete filtered covariance analysis using the Cassini reference trajectory. In contrast to the Europa Clipper analysis, the focus here is on one arc of data, specifically the initial Saturn tour leg, which was designed to target the "Titan-A" flyby occurring about 4 months after SOI. This data arc started shortly after SOI (which occured at approximately 20,000 km altitude) and included an orbit with a high apoapse (9 million km altitude), and three Orbit Trim Maneuvers (OTMs). The first OTM was deterministic and the final two were statistical and used for fine-tuning the Titan flyby. Uncertanties along the arc were computed using simulated optical-only measurements, mapping the results to the Titan B-Plane. The performance at the final two OTMs was then compared to the reference uncertainties used by the mission's Navigation Team. These reference results were primarily radio-based but also included about 340 optical measurements, processed on the ground.[10] The target set for the reference results matches the simulated optical-only target set except that the reference results include Titan but not Phoebe.

Simulated image observables are used in place of the actual images from Cassini's NAC in order to use an optical AutoNav-driven observation schedule. A nominal observation frequency of once per day is assumed, and the frequency changes to every 4 hours in the three days leading up to an OTM or flyby. At each observation time, pictures of up to six moons are taken providing a total of 1,074 optical measurements. With onboard processing of the images, a data cutoff relatively close to the OTM time can be used. We assume a data cutoff 1 hour before each maneuver. In contrast, the radio solutions are processed on the ground leading to a data cutoff about 2 days before each maneuver.

The filter was initialized 16 days after SOI with essentially open *a priori* 1-σ uncertainties of 200 km in each position component and 200 m/s in each velocity component. When the filter is run, the current state knowledge is mapped to the Titan flyby B-Plane assuming any *future* OTMs are executed nominally and do not introduce any uncertainties. At any given time, however, the execution uncertainties for all *previous* OTMs are included in the filtered state uncertainty. The 1-σ semi-major (SMAA) and semi-minor (SMIA) axes on the B-Plane are plotted in Figure 12 along with the 1-σ time of closest approach (TCA). Note that maneuver execution errors introduce a large uncertainty at OTM-2, a large deterministic maneuver with a ΔV of about 393 m/s performed 64 days before Titan flyby. OTM-3 (0.51 m/s, 49 days before flyby) and OTM-4 (0.39 m/s, 3 days before flyby) were much smaller statistical maneuvers and resulted in smaller increases in the mapped uncertainties. Overall, the results show reasonably good improvements in the filter results, with the major axis of the B-Plane ellipse dropping to the 100 km level before OTM-2 and OTM-3 are performed. The performance dramatically improves as Titan is approached, even though Titan itself is not used as a navigation beacon, due to the rich set of satellites available and the correlation between Titan's ephemeris and the target beacons' ephemerides. The B-Plane axes drop to sub-10 km levels prior to the final targeting maneuver.

To visualize the impressive performance of the AutoNav system, Figure 13 compares the 3-σ state uncertainty mapped onto the B-Plane for the filtered optical-only and reference ground-based result at the data cutoffs for OTM-3 and OTM-4 (note that the ground-based solution is labeled "Radio," even though the solution includes some ground-processed optical observations).

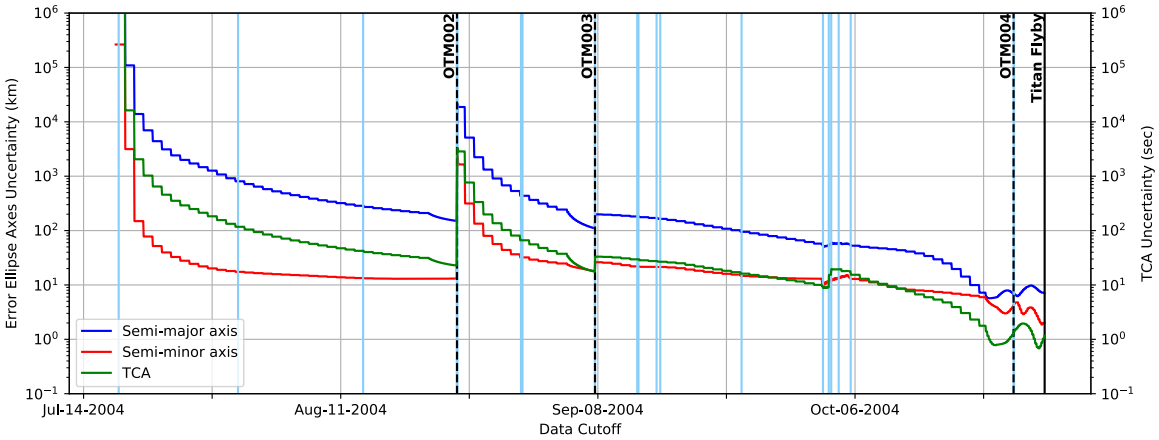

Figure 12. B-Plane 1-σ uncertainties for simulated optical-only approach to Cassini's first targeted Titan flyby. (Light blue lines correspond to times of small velocity perturbations on spacecraft.)

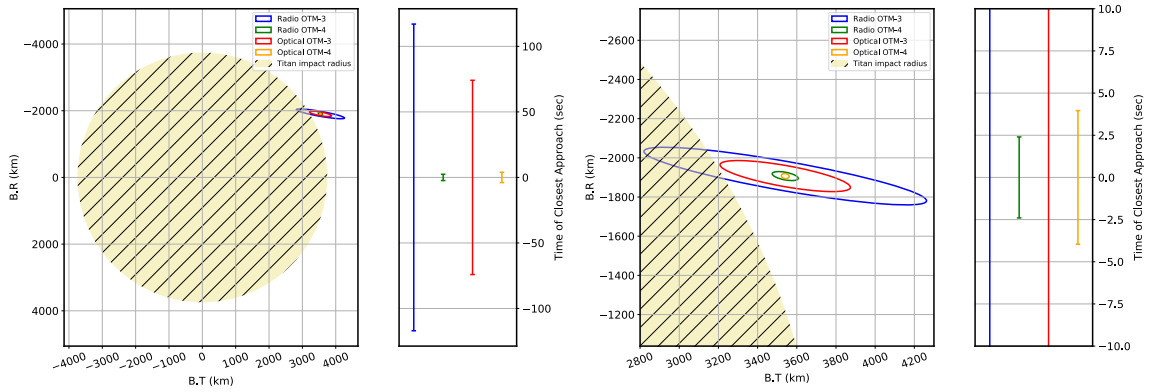

Figure 13. Comparison of B-Plane 3-σ uncertainties at data cutoffs for OTM-3 and OTM-4.

The optical AutoNav solutions at the data cutoffs provide smaller uncertainty ellipses on the B-Plane, though at the OTM-4 data cutoff, the radio solution has a slightly lower TCA uncertainty. In the B-Plane, note that the reference result has the 3-σ ellipse within the impact radius of Titan, which is computed including a 900-km altitude atmosphere, whereas the AutoNav 3-σ ellipse is entirely above the atmospheric impact radius. These results are very promising, suggesting that strictly optical navigation with Cassini's NAC is feasible, at least for this initial Saturn tour leg. We intend to confirm if this performance holds for future legs as well.

CONCLUSION

The performance of an autonomous on-board optical navigation system was evaluated for spacecraft in the vicinity of Jupiter and Saturn. Previous analysis showed that optical-only navigation in deep-space cruise on the way to Jupiter and Saturn may be challenging given the scarcity of visible targets that are suitable for imaging. However, there are possible workarounds, including the addition of small amounts of radiometric data, or simply using "dead-reckoning" navigation until the approach phase for a mission. This possibility can be assessed by performing a full ΔV99 analysis for a specific mission to determine the required statistical fuel allocation.

On approach, the simulated optical measurements are sufficient to support orbit insertion, even with a mid-level camera. The statistical ΔV99 is higher for all cameras than the radio-only results; selectively placed radiometric data could help improve the statistical ΔV margin. Nevertheless, the results indicate that optical AutoNav is viable for orbit insertion at the Gas Giants.

For touring their respective satellite systems, Jupiter and Saturn are a study in contrasts. At Jupiter, the four Galilean satellites are the likely targets for most missions, but these satellites are clustered near Jupiter. Because the accuracy of the optical observations are directly proportional to distance and angular separation, the Jovian system doesn't present much in the way of viable optical targets for performing navigation. The availability of only four candidate targets limits the geometries for imaging opportunities, resulting in somewhat poor results. By contrast, the Saturnian system has a large number of satellites suitably positioned for observations. The rich set means that many choices are available at any given time, and positioning accuracies are in the tens of kilometers for many cases.

These results are borne out when analyzing specific tours as represented by a Europa Clipper reference trajectory and the as-flown Cassini tour. Using optical-only navigation for the Europa Clipper tour may not be feasible without the addition of radiometric data or an improvement in camera technology. With the number of flybys and maneuvers required to complete the tour, the increase in flyby parameter uncertainty with a camera results in significantly higher statistical ΔV costs for all but the highest level of camera with very frequent images. Even with the highest performance for an optical system, the flyby performance is noticeably worse than the radio-only solution.

By contrast, the Cassini mission at Saturn benefits from the number of visible moons, and an optical-only system not only compares favorably to the as-flown mission performance, but even exceeds it in the single case analyzed thus far. This result is very promising, and the next step in the analysis is to verify the performance across the remainder of the tour.

ACKNOWLEDGMENT

The authors would like to thank Sumita Nandi and the Europa Clipper Navigation Team for providing their scripts and setup for navigation covariance analysis, and Julie Bellerose for providing the Cassini setup.

This work was performed at the Jet Propulsion Laboratory, California Institute of Technology, under contract with the National Aeronautics and Space Administration. Government sponsorship acknowledged.

REFERENCES

[1] S. Bhaskaran, "Autonomous Navigation for Deep Space Missions," *Proceedings of the SpaceOps 2012 Conference*, Stockholm, Sweden, June 2012.

[2] S. Broschart, N. Bradley, and S. Bhaskaran, "A Kinematic Approximation of Position Accuracy Achieved using Optical Observations of Distant Asteroids," *Submitted for publication: Journal of Spacecraft and Rockets*, 2018.

[3] S. Broschart, N. Bradley, and S. Bhaskaran, "Optical-Based Kinematic Positioning for Deep-Space Navigation," *Proceedings of the AAS/AIAA Astrodynamics Specialist Conference*, August 2017.

[4] B. Tapley, B. Schutz, and G. Born, *Statistical Orbit Determination*. Elsevier, 2004.

[5] W. Kizner, "A Method of Describing Miss Distances for Lunar and Interplanetary Trajectories," No. JPL External Publication No. 674, 1959.

[6] S. A. Stern, "The New Horizons Pluto Kuiper Belt Mission: An Overview with Historical Context," *Space Science Reviews*, Vol. 140, Jan 2008, pp. 3–21, 10.1007/s11214-007-9295-y.

[7] K.-H. Glassmeier, H. Boehnhardt, D. Koschny, E. Kührt, and I. Richter, "The Rosetta Mission: Flying Towards the Origin of the Solar System," *Space Science Reviews*, Vol. 128, Jan 2007, pp. 1–21, 10.1007/s11214-006-9140-8.

[8] T. Lam, B. Buffington, and S. Campagnola, "A Robust Mission Tour for NASA's Planned Europa Clipper Mission," *2018 Space Flight Mechanics Meeting*, Jan 2018, 10.2514/6.2018-0202.

[9] Z. Tarzi, D. Boone, N. Mastrodemos, S. Nandi, and B. Young, "Orbit Determination Sensitivity Analysis for the Europa Clipper Mission Tour," *29th AAS/AIAA Space Flight Mechanics Meeting (in preparation)*, 2019.

[10] P. Antreasian, J. Bordi, K. Criddle, R. Ionasescu, R. Jacobson, J. Jones, R. MacKenzie, M. Meek, F. Pelletier, D. Roth, I. Roundhill, and J. Stauch, "Cassini Orbit Determination Performance During the First Eight Orbits of the Saturn Satellite Tour," *Proceedings of the 2005 Astrodynamics Specialist Conference*, 2005.